(a) (b) (c) (d) (e)

Figure 6: Segmentation, shape and motion estimation of a human arm. A sample of the image sequence.

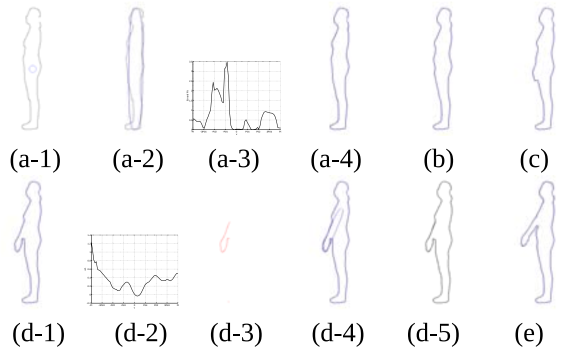

Figure 7: Segmentation, shape and motion estimation of a human arm.

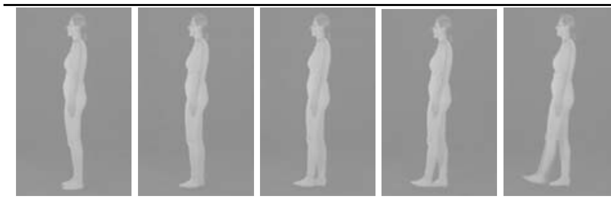

(a) (b) (c) (d) (e)

Figure 8: Segmentation, shape and motion estimation of a human leg. A sample of the image sequence.

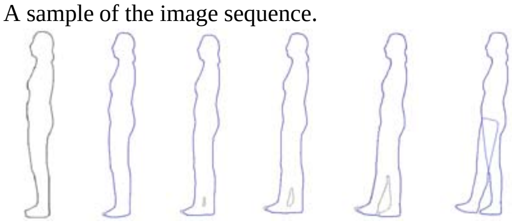

(a) (b) (c) (d) (e) (f)

Figure 9: Segmentation, shape and motion estimation of a human leg.

to our algorithm is a sequence of monocular images from a moving human. In the current work, we restrict ourselves to the following conditions: (1) the individuals are moving in the front-parallel plane of the camera, (2) the individuals wear tight fitting clothes, and (3) the individuals are moving against a stationary background. The first restriction can be overcomed by introducing more sensors (either a pair of stereo cameras or cameras that are organized in a orthogonal configuration in space) which will allow model acquisition and tracking in 3D space. The second condition is necessary in order to acquire the true shape and the parts of the human body. To remove the third constraint, we plan to integrate into our algorithm other visual cues such as color. In this paper, we present the results from observing the actor perform the first phases of motions 2 and 4 from the protocol of motions. The outlines have been obtained by applying a Canny edge detector to the input image sequence. Figs. 6 show six frames from the image sequence. Figs. 7(a-1,a-2) show the initialization of a deformable model, and the fitted model to the first frame using only global deformations. Fig. 7(a-3) depicts the error of fit of the model depicted in Fig. 7(a-2), with respect to the material coordinate v of the geometric primitive. To reliably fit the shape using local deformations, in the areas where the error of fit exceeds a pre-specified threshold, we apply our algorithm for adaptive assignment of data points for large local deformations in the case of static images. Notice that we do not attempt to describe the shape as the result of composition of two primitives since there is no prior motion. Fig. 7(a-4) shows the finally fitted model to the first frame using global and local deformations. Figs. 7(b,c,d-1) show the results of fitting the frames in Figs. 6(b,c,d), respectively. If we plot the profile of the local deformations d_x of the model depicted in Fig. 7(d-1), we obtain Fig. 7(d-2). Fig. 7(d-3) depicts the data that we identify as the projection from another primitive. Fig. 7(d-4) depicts the recovered defining primitives of the composed model. The composed model, depicted in Fig. 7(d-5) is fitted to the data (Fig. 6(d)). Fig. 7(e) shows the fitting of the composed model to the data in Fig. 6(e). In subsequent frames, the Part Decomposition Criterion A is satisfied and we apply the Part Decomposition Algorithm A to recover the underlying parts. Later, joints between the parts are estimated employing the algorithm for joint estimation described in [5].

Figs. 8 show five frames from the image sequence, in which the actor moves her leg. Figs. 9(a-d) depict the models fitted to the data in Figs. 8(a-d). The Part Decomposition Criterion C is satisfied for the the data in Fig. 8(e) so we invoke the Part Decomposition Algorithm C. The models recovered are depicted in Fig. 8(f).

5 Conclusion

We have presented a novel, integrated approach to identifying the parts of a human body and to estimating their shape and motion. Initially, we assumed that the outline is the result of the projection of a single part and we fitted a deformable model to the given data using our physics-based framework. As the actor moved and attained new postures, large protrusions emerged on the outline. To capture the complex shape of the outline, we employed a new representation consisting of composition of deformable models. By monitoring the evolution of shape and motion parameters of